Bulgarian Chemical Communications, Volume 43, Number 1 (pp. 125 – 132) 2011

Synthesis and electrochemical properties of the electrode materials for supercapacitors

M. Mladenov[a*], N. Petrov[b], T. Budinova[b], B. Tsyntsarski[b], T. Petrov[d], D. Kovacheva[c], R. Raicheff[a]

[a]*Institute of Electrochemisty and Energy Systems, Bulgarian Academy of Sciences, Ac. G.Bonchev St., building 10, 1113 Sofia, Bulgaria*
[b]*Institute of Organic Chemistry, Bulgarian Academy of Sciences, Ac. G.Bonchev St., building 9, 1113 Sofia, Bulgaria,*
[c] *Institute of General and Inorganic Chemistry, Bulgarian Academy of Sciences, Ac. G.Bonchev St., building 11, 1113 Sofia, Bulgaria*
[d] *University of Chemical Technology and Metallurgy, 8 St. Kliment Ohridski Blvd., 1756 Sofia, Bulgaria*

Received: August 25, 2010; October 20, 2010

New electrode materials for supercapacitors - activated carbons, produced by carbonization of mixtures of coal tar pitch and furfural, with a subsequent hydrothermal treatment, were characterized and tested electrochemically. The microstructure, surface morphology and porous structure of the carbon materials were studied, and the main textural parameters and micropore size distribution were determined. Symmetric sandwich-type supercapacitor cells, with identical carbon electrodes and organic electrolyte, were assembled and subjected to charge-discharge cycling study at different current rates. Four types of carbons as electrodes with different specific surface area (1000 – 1600 $m^2 g^{-1}$) and texture parameters, as well as tree types of organic electrolytes (Et_4NBF_4 – PC, $LiBF_4$ – PC, $LiPF_6$ – DMC/EC), were tested and compared with an asymmetric supercapacitor, composed by graphitized-activated carbon (carbon foam) as a negative electrode, and activated carbon/$Li_4Ti_5O_{12}$ oxide composite as a positive electrode. The capacitance values of up to 75 $F.g^{-1}$ were obtained for the symmetric supercapacitors, depending on the microstructure and the conductivity of the carbon material, and about two times higher capacitance was obtained for the asymmetric supercapacitor, with good cycleability of both supercapacitor systems.

Keywords: supercapacitors, electrode materials, organic electrolyte, nanostructured carbons, hybrid capacitor

1. INTRODUCTION

In the last years the electrochemical double-layer capacitors (supercapacitors) have attracted worldwide interest of the research groups and companies, working in the field of chemical power sources, due to their potential applications as energy storage devices. In the comparison of different energy storage devices, the batteries show the highest energy density (up to 200 Wh kg^{-1}) but they have low power density (bellow 500 W kg^{-1}) and a limited cycle life (usually less than 1000 cycles). The electrochemical capacitors tend to have lower energy density (up to 10 $Whkg^{-1}$), compared to the batteries, but they can provide high power capability (above 1000 Wkg^{-1}), high reversibility (90–95% or more) and excellent cycling characteristics (usually more than 10^5 cycles). Other advantages of the supercapacitors, compared with the rechargeable batteries, are their extremely low internal resistance, high output power, exceptionally low level of heat emmission while working, and an improved safety. Typically, they exhibit much larger (up to 200 times) capacitance than the conventional capacitors [1–5].

The integration of supercapacitors and batteries in the energy storage systems gives a possibility to combine the high transient performance of the supercapacitors with the high steady-state characteristics of the electrochemical power sources, and thus to attain effective control within the energy storage and consumption processes. The obtained hybrid power source effectively supplies energy for a long time, and in the same time, it is capable to cover high power peaks in both, the consumption and the charging.

Porous carbons are among the most attractive materials for preparation of electrodes for electrochemical capacitors. The main advantage of these materials is the possibility to produce highly porous structures with high specific surface area, and to regulate the porosity texture of the electrodes. On the other hand, the carbon materials give also possibilities to develop various composite electrode structures by adding electrochemically active materials to the carbon matrix [6, 7].

* To whom all correspondence should be sent:
E-mail: mladen47@bas.bg

The electrochemical cells in the carbon-based supercapacitors are usually symmetrical with identical carbon electrodes. In order to improve the energy density while keeping long cycle life, asymmetrical cells, consisting of different types of electrodes, were introduced. Thus, hybrid capacitor configurations, consisting of active carbon as a positive electrode and a negative electrode based on metal oxides (nickel, lead or manganese oxides) [8–10], conducting polymers [11], or Li intercalation oxides [12–13], were suggested, and promising results were obtained. An interesting approach in this respect is also the so called Li ion capacitor, using lithiated graphite and activated carbon for the negative and positive electrodes, respectively [14].

Our previous studies [15, 16] showed that nanoporous carbon materials can be synthesized from waste biomass (apricot stones and spent coffee grounds), and their pore texture could be readily regulated by appropriate thermal and hydrothermal treatment. The electrochemical tests showed promising characteristics (capacity values of up to 60 $F.cm^{-2}$, cycling efficiency of 85–90%) of the symmetrical sandwich-type capacitor cells with tested carbon electrodes and organic electrolyte of Et_4NBF_4 – PC.

The main objective of the this work is to study the electrochemical properties of the newly synthesized carbon electrode materials on the base of waste biomass for supercapacitors. Another aim of this work is to compare the capacitance behaviour of the symmetrical carbon-based supercapacitors with those of the asymmetrical suprecapacitor, composed by carbon and carbon-$Li_4Ti_5O_{12}$ oxide composite electrodes.

2. EXPERIMENTAL

2.1. Synthesis of activated carbons

The mixtures of coal tar pitch and furfural in different proportions (ranging from 30 to 60 wt.%) were treated with concentrated H_2SO_4 (drops of H_2SO_4 were added to the mixtures with continuous stirring) at 120ºC until solidification. The obtained solid product was heated at 600ºC in a covered silica crucible with a heating rate of 10ºC min^{-1} under nitrogen atmosphere. The obtained solid product upon carbonization was further submitted to steam activation at 800ºC for 1 hour for synthesizing the porous carbon. The samples were labelled with C (carbon) and F (furfural) followed by the content in furfural (CF–50 and CF–55). In order to explore the effect of the high temperatures on the electrochemical performance of the carbon materials, selected samples were submitted to an additional heat treatment under nitrogen atmosphere. The CF–50 sample was treated at 1100ºC and the CF–55 sample – at 1400ºC. The samples, submitted to this additional heat treatment, were labelled with H (CF–50H and CF–55H).

2.2. Morphological and physicochemical characterization of the electrode materials

Powder X-ray diffraction spectra were collected within the range from 5 to 80° 2θ, with a constant step of 0.02° 2θ, on Bruker D8 Advance diffractometer with Cu Kα radiation and LynxEye detector. The spectra were evaluated with the Diffrac*plus* EVA and Topas-4.2 packages. The morphology of the activated carbon was examined by means of a scanning electron microscope, the JEOL-Superprobe 733.

The synthesized carbons were characterized by N2 adsorption at −196 ºC, carried out in an automatic volumetric apparatus of ASAP 2020 – Micromeritics. The isotherms were used to calculate the specific surface area, pore volumes and pore size distributions; the latter - using the DFT method.

2.3. Electrochemical tests

The carbon electrodes were prepared from a mixture of 90ºwt.% activated carbon powder and 10ºwt.%. polytetrafluoroethylene (PTFE binder – Aldrich, 60% suspension in water), and pressed on aluminum discs (surface area of 1.75 cm^2). The active material mass was kept constant in all the experiments (15 mg cm^{-2}). The electrodes were soaked in the electrolyte before the cell assembly. The sandwich-type symmetric capacitor cells were constituted of two identical carbon electrodes of comparable mass. The electrodes were electrically isolated by a ceramic-mat separator, soaked with an organic electrolyte, and the cell was assembled in a dry-box under argon. Tree type of organic electrolytes: Et_4NBF_4 – PC (propylene carbonate), $LiBF_4$ – PC and $LiPF_6$ – DMC/EC (dimethyl carbonate/ethylene carbonate in ratio 1:1) (Aldrich p.a.) were used.

The composite electrodes were prepared from electrochemically active nanostructured $Li_4Ti_5O_{12}$ oxide, carbon CF-50 and a conductive material (natural graphite NG–7 or acetylene black), in a 1:1:1 ratio. The asymmetric capacitor cell was composed by activated carbon as a negative electrode and activated carbon-$Li_4Ti_5O_{12}$ composite as a positive electrode with organic electrolyte $LiPF_6$ – DMC/EC.

The capacitor cells were subjected to galvanostatic charge-discharge cycling at different current rates using an Arbin Instrument System BU–2000 [16].

3. RESULTS AND DISCUSSIONS

3.1. Physicochemical characterization

Powder X-Ray diffraction patterns of the CF–50 and CF–55 carbon materials are presented in Fig. 1. Patterns consist of two main amorphous "humps", located at 2θ values of about 24.5º and 43.5º, corresponding to the (002) and (100)+(101) peaks of 2H-hexagonal crystalline graphite. Since carbon materials consist of small packs of graphene sheets, the positions of these two humps show the mean value of the interplanar distances in directions perpendicular to the sheets and within the sheets, correspondingly. The width of the peaks is related to the mean crystallite sizes within the corresponding directions, as presented in Table 1. The pattern of CF–50H sample, which is treated at higher temperature than the CF–50 sample, shows several stronger peaks imposed on the main amorphous-like powder pattern of activated carbon, indicating the formation of graphite domains with higher crystallite sizes.

Table 1. Main parameters obtained from XRD patterns of the carbon samples.

Sample	CF-50	CF-50H		CF-55	CF-55H
	carbon	carbon	graphite	carbon	carbon
(002)-position [A]	3.719	3.732	3.379	3.711	3.684
Distance[nm] between graphene layers [nm]	0.56(6)	0.75(13)	3.23(44)	0.51(9)	0.59(9)
(100)-position [A]	2.081	2.079	2.132	2.083	2.071
Distance[nm] between C atoms in a graphene layer [nm]	0.86(10)	1.42(7)	14(1)	1.23(10)	1.14(8)
		Degree of crystallinity ≈10%			

SEM-photographs of CF–55 sample, prior and upon high temperature thermal treatment, are presented in Fig. 2. No significant changes of the sample morphology are observed.

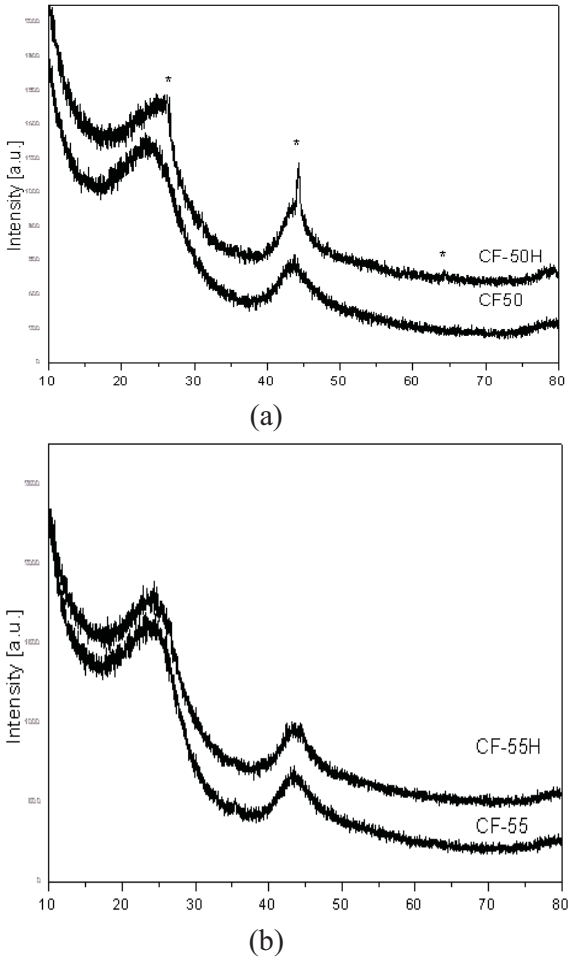

Fig. 1. X-ray diffraction patterns of the activated carbons: a - CF-50 and CF-50H, b - CF-55 and CF-55H.

The pore structure of the carbons was investigated by gas adsorption [17]. The nitrogen adsorption isotherms at –196ºC of the samples were thus recorded (Fig. 3). The main textural parameters of the carbons, obtained from the analysis of the nitrogen adsorption isotherms, are compiled in Table 2. It can be seen from the data in the table that the furfural content has a strong effect on the porosity of the resulting carbons. The sample with the lower proportion of furfural (CF–50) exhibits a type I isotherm according to the BDDT classification, which is indicative for microporous materials. As the content of furfural rises, the isotherms gradually become of the I/IV type, with a clear opening of the knee at low relative pressures. This indicates for development of mesoporosity and widening of the microporosity in the CF–55sample.

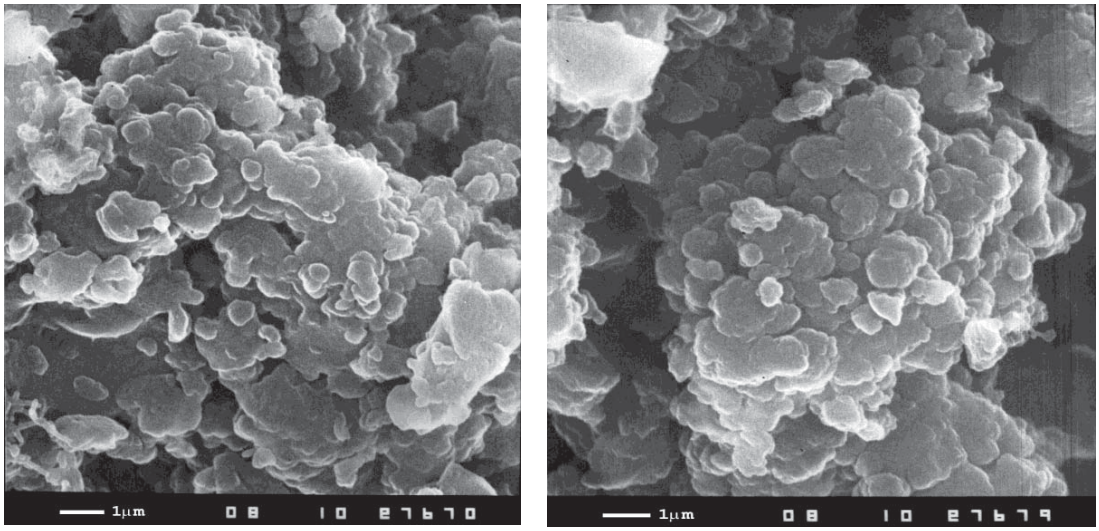

Fig.2. SEM-photograph of carbon samples CF-55 (left) and CF-55H (right).

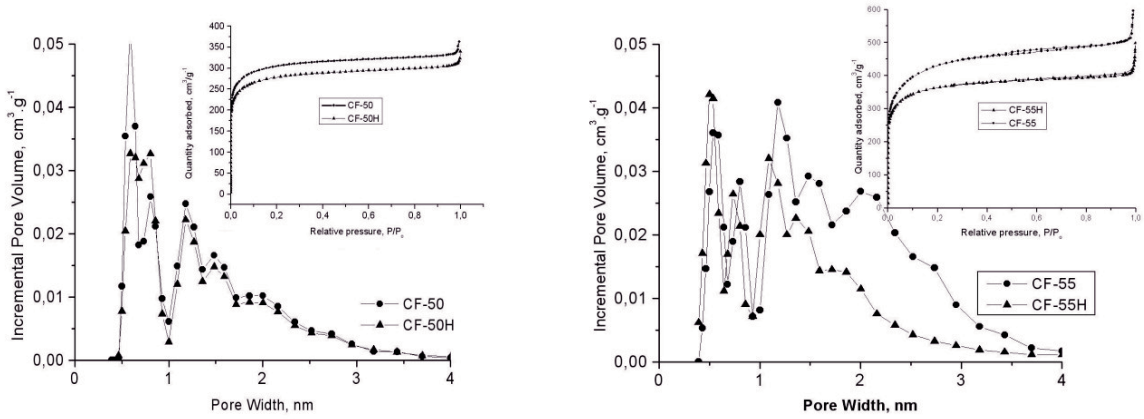

(a) (b)

Fig.3. Pore size distribution and N_2 adsorption isotherms of the activated carbons: a - CF-50 and CF-50H, b - CF-55 and CF-55H.

This observation was confirmed by the analysis of the PSD by the DFT method (Table 2 and Fig.3). Rising the furfural content in the initial mixture from 50% to 55% (CF-50 and CF–55) leads to increase of the micropore and mesopore volumes (cf. Table 2 and Fig. 3). It has been reported that the presence of oxygenated groups enhances the inner resistance and the leakage current of carbon electrodes [18]. Taking into account the large amount of surface oxygen-containing functionalities in the CF-50 and CF-55 carbons, due to the incorporation of furfural in the synthesis [17], it is reasonable to expect a high resistance in these materials. Consequently, carbon samples were submitted to high thermal treatment in order to remove the surface functionalities (CF-50H and CF-55H). On the other hand, it is also known that heating at high temperature may favour internal rearrangements in the carbon structure, which (depending on the carbon precursor) can end up with an increase in the electrical conductivity, if graphite-like domains are formed during the rearrangements. The thermal treatment, however, may also cause some important modifications in the textural and structural properties of the carbon

Table 2. Main textural parameters of the carbons obtained from N_2 adsorption isotherms at -196ºC.

	S_{BET}	V_{TOTAL} [a]	V_{MICRO} [b]	V_{MESO} [b]	Wo N_2 [c]
Samples	$[m^2g^{-1}]$	$[cm^3g^{-1}]$	$[cm^3g^{-1}]$	$[cm^3g^{-1}]$	$[cm^3\ g^{-1}]$
CF-50	1173	0.551	0.374	0.033	0.533
CF-50H	1071	0.486	0.338	0.033	0.473
CF-55	1613	0.761	0.492	0.177	0.604
CF-55H	1397	0.620	0.440	0.074	0.509

[a] evaluated at relative pressures of 0.99
[c] evaluated by DR approach
[b] evaluated by DFT method applied to N_2 adsorption data using slit-shaped pore model

skeleton (annealing effects). Thus it becomes necessary to investigate the porosity of the samples after such a treatment. The results show (Fig. 2) a decrease in the surface area and pore volumes of the treated carbons, which is more strongly expressed in the case of CF–55H (treated at a higher temperature), and more precisely for the mesopore volume.

3.2. Electrochemical performance

Two-electrode symmetric cells were used to evaluate the electrochemical characteristics of the carbon electrode material of CF-50 in different electrolytes: Et_4NBF_4 – PC, $LiBF_4$ – PC and $LiBF_6$ – DMC/EC. The discharge capacities of the capacitors with different electrolytes are compared at different current rates (20 – 160 mA g^{-1}), in the potential range between 1.2 and 2.5 V, Fig. 4. As we can see, the capacity of CF-50 electrodes decreases gradually with the increase of the discharge current in all electrolytes, but this decrease is more pronounced for capacitors with electrolytes, containing Li^+ ions. At low current rates (e.g. at about 20 mA g^{-1}) all three types of capacitors have very close capacity values. At high current rates, however, the capacitors with Li^+ ions in the electrolyte demonstrate quite different behavior in comparison with the capacitor cell with Et_4N^+ in the electrolyte, as the capacitance of the latter is much higher than those of the other two cells. Thus, the discharge capacity values of the carbon-based symmetric capacitors, depending on the employed organic electrolyte, can be ranked in the following order: Et_4NBF_4 > $LiBF_4$ >$LiPF_6$. The effect of the electrolyte on the discharge capacity may be related to the dimensions of the solvating 'guest' ions in the electrolyte. Additional investigation, however, is required in order to elucidate quantitatively the above effect. In the following electrochemical studies on the carbon electrode materials, Et_4NBF_4 – PC was used as electrolyte in the capacitor cells.

The good cycleability of all three capacitors is illustrated in Fig.4. It shows the charge-discharge profiles of the capacitors after 50 cycles. The cell, using Et_4NBF_4 electrolyte, demonstrates not only the highest capacity but the most stable cycleability as well. It should be noticed that the capacitor cells, using Li^+-base electrolyte, have not such high capacitance as expected, and moreover, their cycling performance is not so stable, especially at high current rates, as compared to this of the cell with Et_4N^+– based electrolyte. Two-electrode symmetric capacitor cells were assembled with various active carbon materials (CF–50, CF–50H, CF–55 and CF-55H) as well as asymmetric capacitor cells, constituted by activated carbon (CF-50) and composite electrode (carbon CF–50/ $Li_4Ti_5O_{12}$ oxide with additive of natural graphite NG–7).

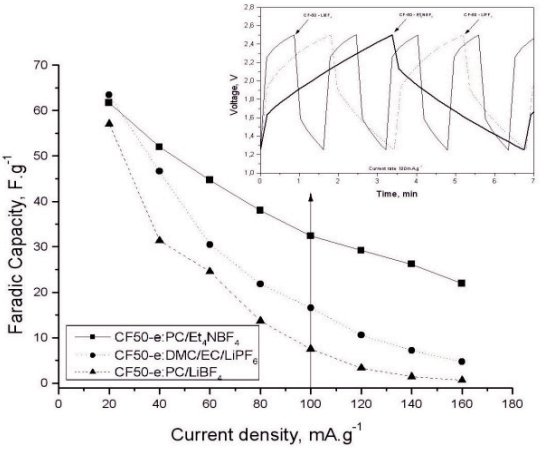

Fig. 4. Dependence of capacity on discharge current and cycling performance for symmetric cells carbon CF–50 and different electrolytes.

The PTFE content in the active material was kept constant (10 wt.%), and the organic electrolyte was of 1.5 M Et_4NBF_4 in PC in all cases. The cells thus composed were subjected to galvanostatic cycling at different current rates (20 – 160 m Ag^{-1}).

The capacitance of the capacitor cell was calculated from the slope of the potential – time (V–t) curves:

$$C=I/(dV/dt) \quad (1)$$

where C is the capacitance of the cell (F), I is the discharge current (A), and dV/dt is the slope of V-t curve (V.s^{-1}).

In a symmetric cell, the specific capacitance Cm_{AM} (capacitance per unit mass activated carbon material, F.g^{-1}) is related to the capacitance of the cell C and the carbon mass m_{AM} by the following equation:

$$Cm_{AM}=2C/m_{AM} \quad (2)$$

Fig.5 presents typical capacity-current rate plots, obtained during galvanostatic charge/discharge cycling of different capacitor cells. We can seen that all carbons show satisfactory capability of charge accumulation in the electric double layer up to current rates of about 150-160 mA.g^{-1}. The capacitance values of the cell with carbon electrodes of CF-50 (S_{BET} = 1170 $m^2.g^{-1}$, V_M =

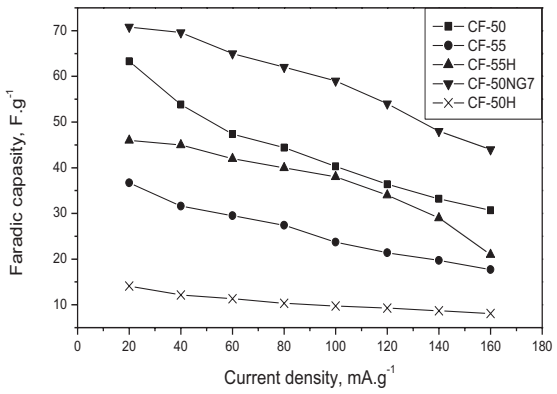

Fig. 5. Dependence of capacity on discharge current for symmetric cells with different carbons and Et_4NBF_4 electrolyte (CF-50NG7 – carbon CF-50 with an addition of 10% natural graphite NG-7).

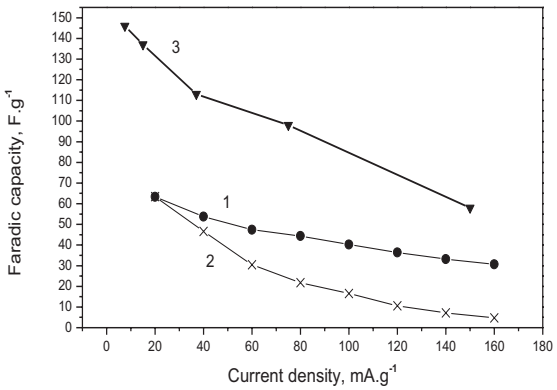

Fig. 6. Dependence of capacity on discharge current for symmetric cells (1- CF-50 – Et_4NBF_4 and 2- CF-50 – $LiPF_6$) and asymmetric cell (3- CF-50/composite CF-50 + $Li_4Ti_5O_{12}$ - $LiPF_6$).

0.374 $cm^3.g^{-1}$), however, are much higher than those of the cell with carbon electrodes of CF-55 (S_{BET} =1600 $m^2.g^-1$, V_M= 0.492 $cm^3.g^{-1}$). It is usually anticipated that the capacitance of the porous carbon should be proportional to its available surface-area [19]. In practice, the major factors that contribute to this relationship, often with a complex non-linear character, are: the assumptions in the measurement of electrode surface-area, variations in the specific capacitance with differing morphology and pore-size distribution, variation in surface chemistry, conductivity of the carbon particles, etc. The activated carbons of CF–50 and CF–55 show quite different porous texture characteristics: pore volume, surface-area, and micropore size distribution (cf. Table 2 and Fig. 3).

There are contradictory reports in the literature on the effect of increasing surface area and porosity on the intrinsic electronic conductivity of compact carbon powders [19]. It seems logical to expect that the volumetric conductivity decreases as the microporosity (V_M) and surface area (S_{BET}) increase. In this respect, the results of some authors [17] show that the specific resistance of the cell, using activated carbon CF–50, is 0.8 Ω cm^2, and 1.2 Ω cm^2 for the cell, using CF–55 carbon. In this comparison, the higher capacitance values of the cell with CF-50 carbon (30% more than the capacitance of the cell with CF-55 carbon, with the same electrolyte Et_4NBF_4 – PC) is most probably due to its higher conductivity.

As mentioned above, the presence of oxygenated groups in the carbons of CF–50 and CF–55 enhances their inner electroresistance. Consequently, these carbons were submitted to thermal treatment at high temperature in order to remove the surface functionalities. Fig.1 and Table 1 show that this treatment leads to rearrangements in the carbon structure and graphitic-like domains are formed, proved by XRD analysis of the CF–50H (around 10% degree of crystallinity) and the CF–55H carbons. Depending on the carbon precursor this process can end up with an increase in the electrical conductivity and its Faradic capacity. The results in Fig. 5 show that the capacity of the CF–55 carbon increases after heat treatment (CF-55H), but the capacity of the CF–50 carbon at these conditions drastically decreases, and the cell using CF-50H carbon as electrodes demonstrates rather poor bevaviour (capacity values 10–15 $F.g^{-1}$ in the whole current range). It is possible to assume that during this treatment some rearrangements may occur in the CF–55 carbon, which results in important modifications in the textural and the structural properties of the carbon skeleton (annealing effects) – cf. Fig.1, Table 2, Fig.3

The addition of natural graphite, NG–7 (10 w%), to the CF-50 carbon decreases the specific resistance of the electrode from 0.8 down to 0.5 Ω cm^2 , thus increasing the electronic percolation [17]. As a result, the cell, using carbon material CF–50NG7 as electrodes, shows the best performance - capacitance value up to 75 $F.g^{-1}$ at 20 $mA.g^{-1}$ and satisfactory one (about 50 $F.g^{-1}$) at 160 $mA.g^{-1}$ (cf. Fig.5).

Fig.6 illustrates the dependence of the specific capacitance on the discharge current for symmetric carbon-based (CF-50) capacitors with Et_4NBF_4 – PC or $LiPF_6$ – DMC/EC electrolytes, and an asymmetric capacitor, composed by graphitized

carbon (CF-50H) as negative electrode and composite carbon CF-50 – $Li_4Ti_5O_{12}$ oxide as positive electrode with $LiPF_6$ – DMC/EC electrolyte. As expected, the capacity of the symmetric capacitor cell with Li^+-based electrolyte is lower than this of the capacitor with Et_4NBF_4 electrolyte. The comparison of the capacity-discharge current plots shows also that the asymmetric capacitor demonstrates near twice as higher capacitance (up to 150 $F.g^{-1}$) than those of the best symmetric one (up to 70 $F.g^{-1}$) at all current rates. The higher capacitance values of the asymmetric capacitor could be explained with the occurrence of the process of intercalation of solvated Li^+ ions into graphitized carbon and carbon – $Li_4Ti_5O_{12}$ composite electrodes together with the ion adsorption.

4. CONCLUSIONS

Based on the current study results, the following conclusions could be made:

a) New electrode materials for supercapacitors - activated nanostructured carbons are synthesized by carbonization of mixtures of coal tar pitch and furfural with subsequent hydrothermal treatment, and characterized physicochemically.

b) Composite electrodes for supercapacitors are produced from activated carbons, nanostructured electrochemically active $Li_4Ti_5O_{12}$ oxide and a conductive additive (natural graphite NG–7 or acetylene black).

c) The organic electrolyte plays a very important role in the determination of the capacity performance of the symmetric carbon-based supercapacitors.

d) The conductivity, the pore size distribution and the chemical surface properties of the carbon materials contribute greatly to the charge storage behaviour of the electrodes in the symmetric supercapacitors.

e) The capacitance values of up to 75 $F.g^{-1}$ are obtained for the symmetric carbon-based supercapacitors with Et_4NBF_4 – PC electrolyte and about twice as higher capacitance for the asymmetric supercapacitor, composed by graphitized carbon as a negative electrode and carbon-$Li_4Ti_5O_{12}$ oxide composite as a positive electrode in $LiPF_6$ – DMC/EC electrolyte, with good cycleability of both supercapacitor systems.

Acknowledgment: *This work is supported by the Bulgarian NSF under the TK–X–1705 / 2007 Project.*

REFERENCES

1. B.E. Conway, Electrochemical Supercapacitors: Scientigic Fundamentals and Technological Applications, Kluwer Academic Publ., New York, 1999.
2. V. Khomenko, E. Raymundo-Pinero, F. Beguin, *J. Power Sources,* **177**, 643 (2008).
3 .Y. Zhang, H. Feng, X. Wu, L. Wang, A. Zhang, T. Xia, H. Dong, V. Li, L. Zhang, Intern. *J. Hydrogen Energ*., **34**, 4889 (2009).
4. J.Gamby, P. L.Taberna, P. Simon, J. F. Fanvarue, M. Chesnean*, J. Power Sources* **101,** 109 (2001).
5. A.Brucke, *J. Power Sources*, **91**, 37 (2000).
6. R. Kotz, M. Carlen, *Electrochim. Acta* **45,** 2483 (2000).
7. R.S. Brood, K.R Bulock, R.A.Leising, R.L.Middouh, J.R. Miller, E. Takeuchi, *J. Electrochem.Soc.* **151,** LOK1 (2002).
8. S. Razumov, A. Klementov, S. Letvinenko, A. Beliakov, *US Patent* 6,222,723 (2001)
9 .W. G. Pell, B. E. Conway, *J. Power Sources,* **136,** 334 (2004).
10.V. Khomenko, E. Raymundo-Pinero, F. Beguin, *J. Power Sources,* **153**, 183 (2006).
11. C.A. Fabio, A. Giorgi, M. Mastragostino, F. Soavi, *J. Electrochem. Soc*., **148,** A845 (2001).
12. G. G. Amatucci, F. Badway, A. Du Pasquier, T. Zheng, *J. Electrochem Soc*., **148,** A930 (2001).
13. A. Du Pasquier, I. Blitz, J. Gural, S. Menocal, G.G. Amatucci, *J. Power Sources,* **143,** 62 (2003).
14. V. Khomenko, E. Raymundo-Pinero, F. Beguin, *J. Power Sources,* **177**, 643 (2008).
15. M. Mladenov, P. Zlatilova, R. Raicheff, S. Vassilev, N. Petrov, K. Belov, V. Trenev, *Bulg. Chem. Commun.,* **40**, 360 (2008).
16. M. Mladenov, R. Raicheff, N. Petrov, D. Kovacheva, R. Nickolov, V. Trenev, D. Bachvarov , K.Belov, *Proc. 4M/ICOMM 2009 Conference*, Karlsrhue, Germany (2009) 223
17. B. Petrova, B. Tsyntsarski, T. Budinova, N. Petrov, C.O. Ania, J.B. Parra, M. Mladenov, P. Tzvetkov, *Fuel Process. Technol*. (2010), doi: 10.1016/j.fuproc.2010.07.008
18. H. Wang, M.Yoshio, *Electrochem. Commun*. **10**, 382 (2008).
19. K.Naoi, A. Nishino, T. Morinoto (Eds), *Electro-chemical Capacitors Compact Dictionary*, **NTS**, 2004, 89.

СИНТЕЗ И ЕЛЕКТРОХИМИЧНИ СВОЙСТВА НА ЕЛЕКТРОДНИ МАТЕРИАЛИ ЗА СУПЕРКОНДЕНЗАТОРИ

М. Младенов[a], Н. Петров[в], Т. Будинова[в], Б. Цинцарски[в], Т. Петров[d], Д. Ковачева[c], Р. Райчев[a]

[a] *Институт по електрохимия и енергийни системи, Българска академия на науките, ул. Ак. Г. Бончев, бл. 10, 1113 София,*

[в] *Институт по органична химия, Българска академия на науките, ул. Ак. Г. Бончев, бл. 9, 1113 София*

[c] *Институт по обща и неорганична химия, Българска академия на науките, ул. Ак. Г. Бончев, бл. 11, 1113 София*

[d] *Химико-технологичен и металургичен университет, бул. Кл. Охридски, 1756 София*

Постъпила на 25 Август, 2010 г.; преработена на 20 Октомври, 2010 г.

(Резюме)

Синтезирани са нови електродни материали за суперкондензатори- активни въглени, получени чрез карбонизация на смеси от каменовъглен пек и фурфурал, с последваща хидротермална обработка. Изследвани са микроструктурата, повърхностната морфология и структурата на порите на получените въглеродни материали и са определени техните основни текстурни параметри и разпределението на порите по размери. Разработени са симетрични суперкондензаторни клетки (тип „ сандвич”) с еднакви въгленови електроди и органичен електролит, които са подложени на зарядно-разрядно циклиране с различни плътности на тока. Като електроди са тествани четири вида въгленови материали с различна специфична повърхност (1000 – 1600 m^2g^{-1}), както и три вида органични електролити (Et_4NBF_4- PC, $LiBF_4$- PC и $LiPF_6$ – DMC/EC). Работата на симетричните суперкондензатори е сравнена с тази на асиметричен тип суперкондензатор, съставен от активен въглен (въгленова пяна) като положителен електрод и композит – активен въглен / $Li_4Ti_5O_{12}$ оксид, като отрицателен електрод. Получени са стойности на капацитета до 75 Fg^{-1} за симетричните суперкондензатори и 2 пъти по-високи стойности за асиметричния суперкондензатор, при много добра циклируемост и за двата типа електроди.